Seeing Molecules from Space: Tools for optically estimating CDOM composition

Brice Grunert[1], Colleen Mouw[2], Karl Meingast[1], Audrey Ciochetto[2]

[1] Michigan Technological University

[2] The University of Rhode Island

Introduction

Study Concept

Colored dissolved organic matter (CDOM) absorption (a_{CDOM}) varies significantly due to differences in source material, degradation pathways and *in situ* production. Satellite remote sensing provides a platform to observe this variability over broad spatial scales and time.

Problem

Current and near future sensors are/will be limited to measurements within the UV and visible wavelengths (> 350 nm) while most optical proxies estimating CDOM composition use wavelengths < 350 nm.

Science Questions

SQ1) Can we identify different types of CDOM using optical metrics?

SQ2) Can we discern any of these differences from a hyperspectral satellite sensor?

Methods

In Situ Data: Absorption spectra were fitted using a Gaussian decomposition approach (Fig. 2a,b). Fitted Gaussian components were aggregated and clustered using a k-means cluster analysis as guidance, with location, width and normalized peak height (peak height/baseline absorption at peak location) as the basis for clustering (Fig. 3). Fluorescence peaks C and A were delineated as described in Coble (1996). *Hydrolight*: Initial remotely-sensed reflectance ($R_{rs}(\lambda)$) was simulated using *in situ* absorption and scattering data. For each sampling site, $S_{350:550}$ was calculated and a_{CDOM} spectra were simulated using observed $S_{350:550}$ ± 0.005 in 0.001 increments. We utilized initial λ values of 350, 400, 450 and 500 nm and utilized the average CDOM absorption as input to simulate differences in $R_{rs}(\lambda)$ due to changes in S_{CDOM}.

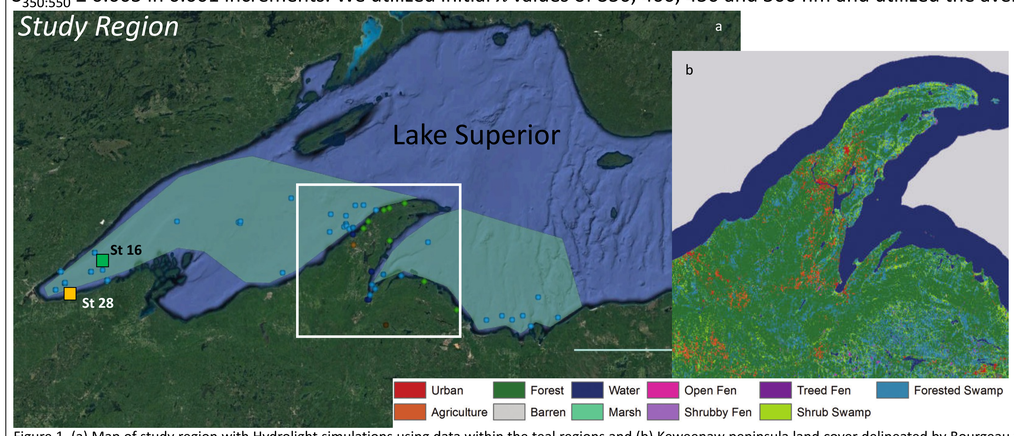

Figure 1. (a) Map of study region with Hydrolight simulations using data within the teal regions and (b) Keweenaw peninsula land cover delineated by Bourgeau-Chavez et al. 2017. The green and gold boxes correspond to highlighted Hydrolight stations. Green dots indicate sampled river systems, blue dots lake stations, and brown dots study sites for soil samples.

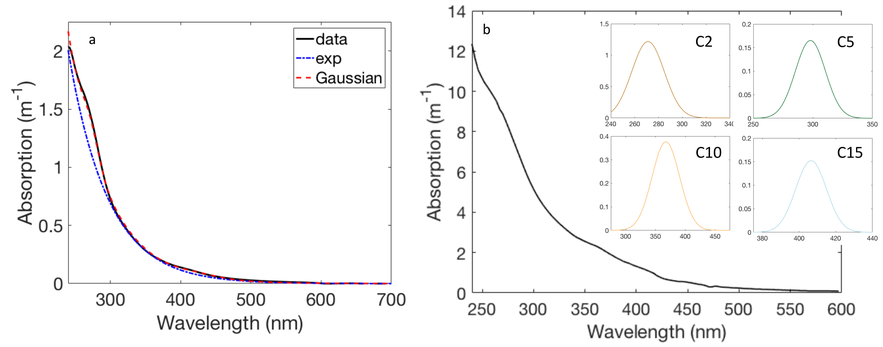

Figure 2. (a) Example spectra fitted using a standard exponential expression and a Gaussian decomposition approach (from Grunert et al. 2018). (b) Example spectra from this dataset showing raw data and the respective fitted components using identified components from Fig. 3.

CDOM Optical Variability Across Different Environments

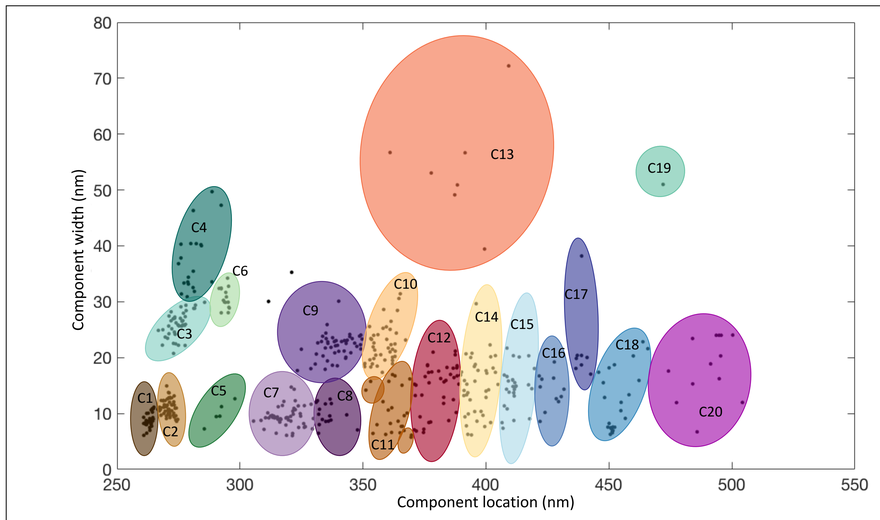

Figure 3. Component clusters identified using k-means cluster analysis. Cluster analysis was performed on component location, width and normalized peak height (Grunert et al. 2018). Location and width were not normalized, resulting in a hierarchy of importance for clustering of location, width then normalized peak height. Clusters defined here are used to identify components in Fig. 4-6.

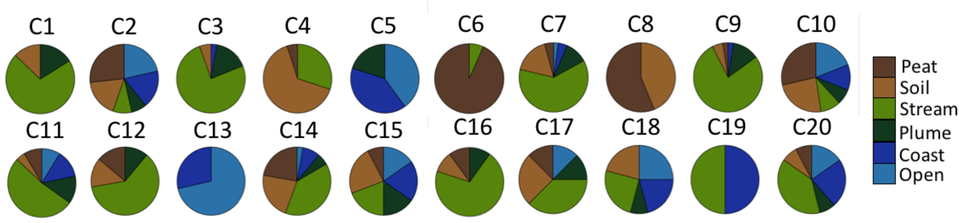

Figure 5. Samples were delineated based on the environment sampled: soil pore water from peatlands (peat) or forested watersheds (soil), streams (reach < 25 km), plume (of sampled streams), coastal Lake Superior (depth < 20 m) and open Lake Superior (depth > 20 m). Each chart represents the ecotype membership for that component. Key findings: C1, C9, C12, C16 appears to be a microbial product of soils or soil/stream systems, C5/C13 appear to be a product of coastal priming or production, C6 is almost exclusively limited to peatlands (1 pre-thaw soil sample) potentially derived from a different type of lignin or degradation pathway, and C8 is exclusive to soil pore water, likely a non-photodegraded microbial byproduct. We suggest that components identified in all ecotypes are microbial byproducts ubiquitous to most ecosystems or terrestrial compounds resistant to degradation. These compounds may be photorefractory in nature or are structurally complex in the case of lignin (e.g. C2).

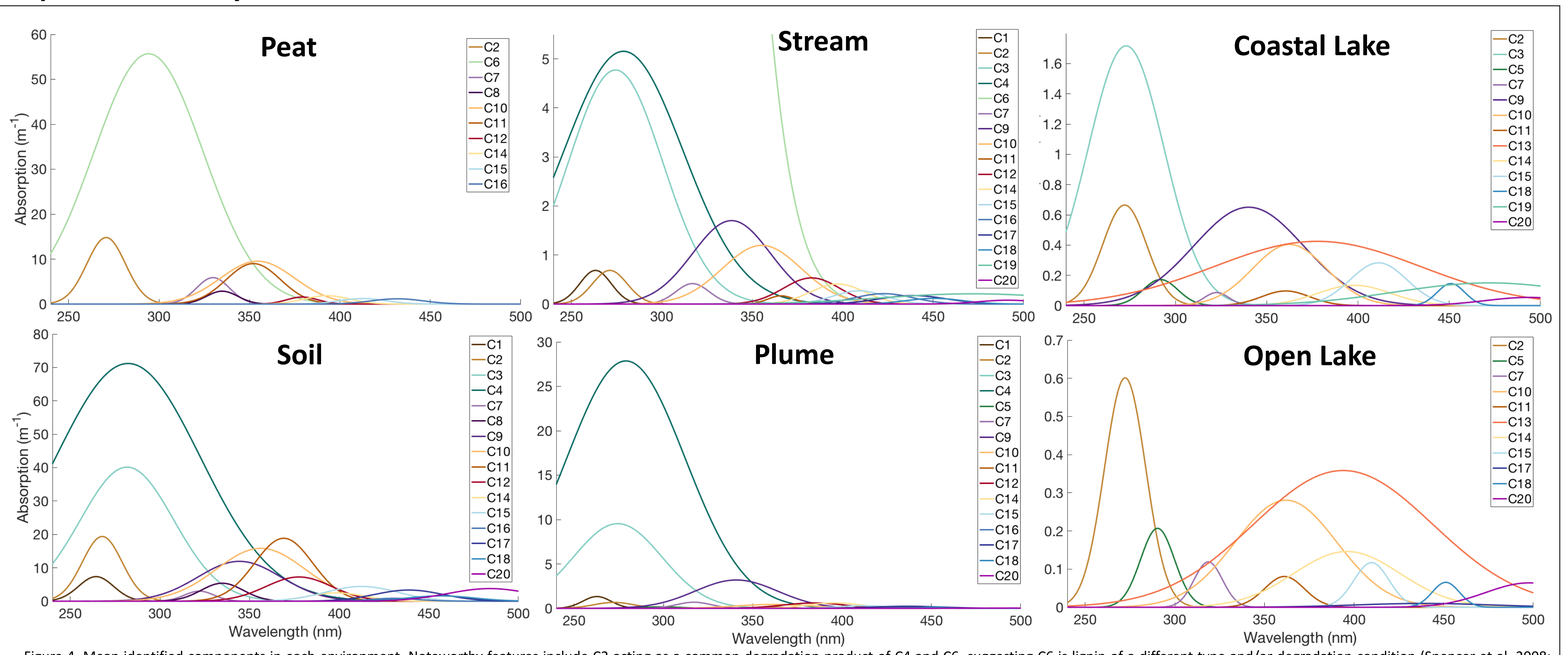

Figure 4. Mean identified components in each environment. Noteworthy features include C2 acting as a common degradation product of C4 and C6, suggesting C6 is lignin of a different type and/or degradation condition (Spencer et al. 2008; Schellekens et al. 2015). As found in Grunert et al. (2018), lignin components and their derivatives largely influence spectra at short wavelengths, while components identified in coastal and open lake systems were of a similar magnitude regardless of spectral location, suggesting optical variability in these samples is driven by longer wavelength components. We note that this is consistent with a charge-transfer model for a_{CDOM}, with the exception that individual chromophores at λ > 375 nm are present, and contribute significantly to autochthonously produced CDOM. This is consistent with the findings of Catalá et al. (2016).

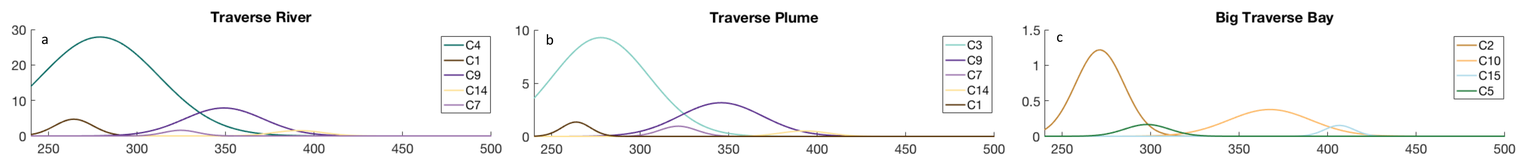

Figure 6. Example of within system consistency for Gaussian components. The peak designated as lignin absorption shows a shift from C4 within the river (a) to C3 in the plume (b) to C2 in the coastal environment (c). This change is tracked both by a blue-shift in component location as well as a decrease in component width and height. C1, C7 and C9 blue-shifted and decreased in magnitude, while C14 red-shifted and decreased in magnitude from river to plume. Within the coastal environment, wholly different components were identified.

Traditional Metrics Across Different Environments

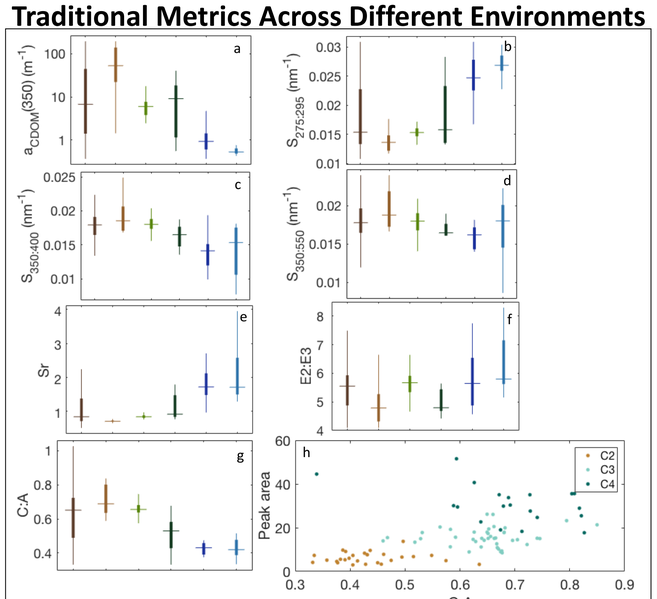

Figure 7. Mean and distribution for each ecotype following the same color scheme as Fig. 5 for (a) $a_{CDOM}(350)$, (b) $S_{275:295}$, (c) $S_{350:400}$, (d) $S_{350:550}$, (e) slope ratio (S_r), (f) E_2:E_3 ($a_{CDOM}(250)/a_{CDOM}(365)$) and (g) fluorescence peak C:A ratio. Fluorescence index (FI), humification index (HIX) and biological index (BIX) were also considered but were not significantly different across environments. Spectral slope followed typical trends observed across terrestrial to aquatic gradients, with open lake $S_{350:400}$ and $S_{350:550}$ displaying a relatively large range and a mean that differs at a magnitude visible to NASA's proposed PACE sensor (see Fig. 8). E_2:E_3 values were within the range of Suwannee River fulvic acid suggesting a relatively low electron accepting capacity (Sharpless et al. 2014), while C:A values suggest a consistent degradation of relatively fresh terrestrial material from soils to the open lake. (h) Displays the relationships between C:A and normalized peak area for components identified as lignin within this dataset, suggesting consistency between these metrics.

Hydrolight Simulations

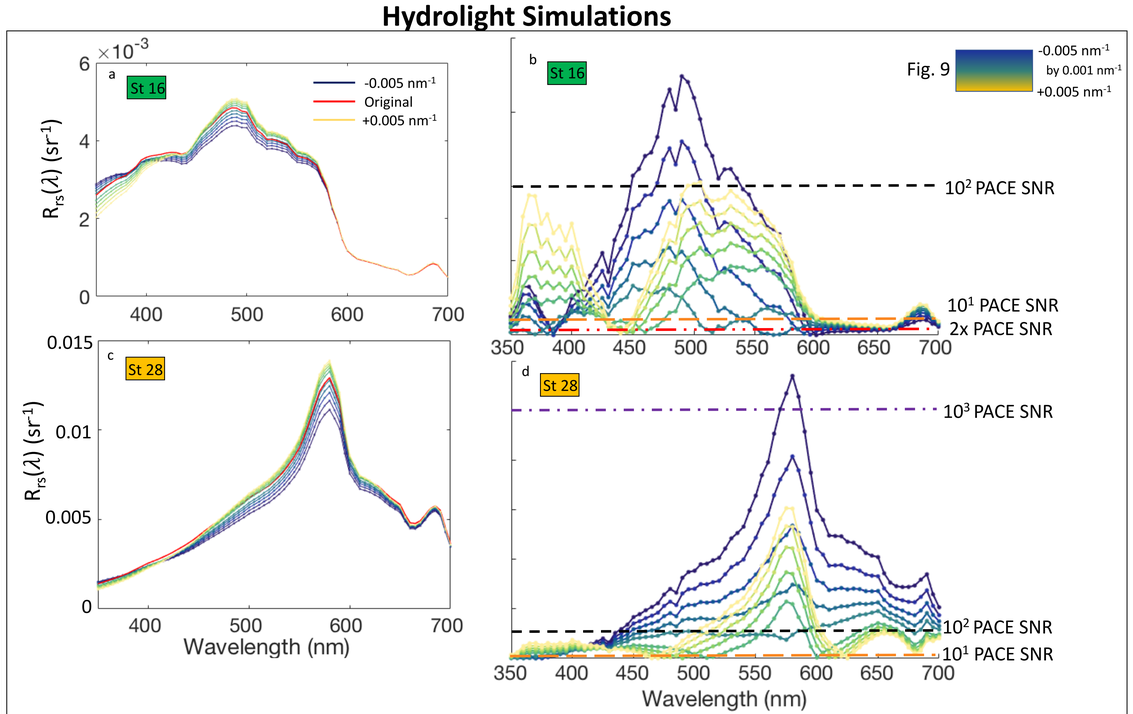

Figure 8. Difference between the initial simulated R_{rs} (red line) and simulated R_{rs} ($S_{350:550}$ original ±0.005 nm^{-1} in 0.001 nm^{-1} increments reflective of *in situ* variability across stations) was calculated from spectra in (a) for Station 16 and in (c) for Station 28. These changes were divided by the signal-to-noise (SNR) ratio of NASA's proposed PACE sensor for (b) Station 16 and (d) Station 28. Points where lines touch the x-axis indicate differences below PACE's SNR at that wavelength. For all simulations, PACE will be capable of detecting changes in $S_{350:550}$ with adequate atmospheric correction at most wavelengths. As shown in Fig. 7, $S_{350:550}$ varies across environments and within the open lake at levels greater than 0.001 nm^{-1}. From this, we would expect to directly estimate changes in CDOM composition affiliated with $S_{350:550}$ variability in Lake Superior using PACE.

Conclusions

SQ1: Yes, we found consistent differences between CDOM from different environments using optical metrics. $S_{350:550}$ variability in open lake samples appears to be driven by absorbing components at wavelengths > 350 nm. These components contribute proportionally more to the absorption spectrum than these components do in terrestrial samples when present.

SQ2: $S_{350:400}$ and $S_{350:550}$ differ at a large enough magnitude between environments to infer changes in CDOM composition from a satellite sensor. Importantly, we point out a mechanistic process for variability in this region of the spectrum.

Gaussian components suggest that within system optical variability in terrestrial samples is driven by changes to short wavelength components while optical variability in aquatic samples is driven by changes in long wavelength components.

Variability in $S_{350:400}$ and $S_{350:550}$ in Lake Superior samples is viewable by PACE for simulated conditions, with links to changes in CDOM composition through the addition and loss of long wavelength absorbing components.

Acknowledgements: Thank you to Amy Marcarelli, Ashley Coble and Evan Kane for data collection.

Citations: Bourgeau-Chavez et al. 2017 *Can. J. For. Res.*, 47; Catalá et al. 2018 *Geophys. Res. Lett.*, 43; Coble 1996 *Marine Chemistry* 51; Grunert et al. 2018 *Global Biogeochemical Cycles*, 32; Schellekens et al. 2015 Geoderma, 237-238; Sharpless et al. 2014 Env. Sci. Tech., 48; Spencer et al. 2008 *Global Biogeochemical Cycles*, 22

Supported by a NASA Earth and Space Science Fellowship (NESSF)